Ceramics International 49 (2023) 18228–18237

Contents lists available at ScienceDirect

Ceramics International

journal homepage: www.elsevier.com/locate/ceramint

Effect of moisture on the reactivity of alpha-tricalcium phosphate

Montserrat Espanol [a,b,*], Emilia Davis [a], Eliott Meslet [a], Gemma Mestres [a], Edgar B. Montufar [a,1], Maria-Pau Ginebra [a,b,c]

[a] Biomaterials, Biomechanics and Tissue Engineering Group, Department of Materials Science and Metallurgical Engineering, Universitat Politècnica de Catalunya, Avinguda Eduard Maristany 16, 08019, Barcelona, Spain
[b] Barcelona Research Center in Multiscale Science and Engineering, Universitat Politècnica de Catalunya, Avinguda Eduard Maristany 16, 08019, Barcelona, Spain
[c] Institute for Bioengineering of Catalonia (IBEC), 08028, Barcelona, Spain

ARTICLE INFO

Keywords:
Moisture
Alpha-tricalcium phosphate
Relative humidity
Vapor sorption
Hydrolysis

ABSTRACT

The ability of the high-temperature polymorph of tricalcium phosphate, α-TCP, to hydrolyse to calcium-deficient hydroxyapatite underlies many developments in the field of synthetic bone grafts, including calcium phosphate cements, foams, and self-setting inks. The objective of the present work was to investigate the effect of humidity on α-TCP powder reactivity. The results showed that a 3-week incubation at high relative humidity (80%) had no impact on reactivity, but, as the incubation was prolonged, the powder started to hydrolyse. This reactivity was associated to the presence of defects and to an amorphous phase induced during powder milling. Moisture studies performed under static/dynamic conditions gave comparable water adsorption percentages. The dynamic studies further proved irreversible water sorption, indicating that some water molecules reacted with the powder after short incubation times. Taken together, these results demonstrate that, although α-TCP powder adsorbs water from moisture immediately, the impact on reactivity appears only after several weeks of storage.

1. Introduction

The first publication on the use of calcium phosphates for bone regeneration dates back to 1920 [1]. Since then, calcium phosphates and, particularly, α-tricalcium phosphate (α-TCP), have been the focus of extensive research. A very promising application of α-TCP is in the formulation of hydraulic bone cements [2,3]. More recently, α-TCP combined with hydrogels has gained interest in the formulation of injectable self-setting inks for applications in minimally invasive surgery and in the field of 3D-printing for the design of personalized bone grafts [4–6]. In all these applications α-TCP powder is brought into contact with water to trigger its hydrolysis reaction. The outcome of the reaction is the precipitation of a network of calcium deficient hydroxyapatite (CDHA) crystals similar in composition to the bone mineral phase. However, the setting reaction is not instantaneous, and the reaction proceeds forming an initial mouldable plastic paste that gradually hardens by the entanglement of the precipitating crystals [7]. The control of the reaction kinetics is crucial in all the above mentioned applications, and particularly for 3D printing, where the rheology of the self-setting ink is controlled by the powder reactivity. There are various strategies that can be used to tune the setting of cements and these typically include adding accelerants and nucleation seeds in the cement formulation or the modification of α-TCP features such as the particle size, crystallinity and the content of amorphous phase [8–10].

In these last years there has been substantial interest to explore the potential of altering α-TCP features to manipulate the cements' reactivity [8,9,11]. In the works of Durucan and Brown [12] and Ginebra et al. [13] α-TCP was milled with different protocols to produce powders with different particle sizes, hence different reactivities. Gbureck et al. [14] proved that besides a reduction in particle size, the prolonged milling of α-TCP induced the formation of an amorphous phase in the powder causing a drastic increase in reactivity. Camiré et al. [15] studied in detail the influence of milling of α-TCP on the powder reactivity and concluded that the increased reactivity was mostly due to the presence of amorphous phase rather than the reduction in particle size or the increase in specific surface area. Later studies by Hurle et al. [16] found that the amorphous phase reacts first, followed then by crystalline α-TCP and determined the reaction enthalpies which allowed to estimate

* Corresponding author. Biomaterials, Biomechanics and Tissue Engineering Group, Department of Materials Science and Engineering, Universitat Politècnica de Catalunya, Avinguda Eduard Maristany 16, 08019, Barcelona, Spain.
E-mail address: montserrat.espanol@upc.edu (M. Espanol).
[1] Present address: Central European Institute of Technology, Brno University of Technology, Purkyňova 123, Brno 612 00, Czech Republic.

https://doi.org/10.1016/j.ceramint.2023.02.193
Received 3 September 2022; Received in revised form 16 February 2023; Accepted 22 February 2023
Available online 26 February 2023

the heat release to the surrounding tissue during the cement setting reaction [17].

Despite the wealth of data on the control of the reactivity of α-TCP in water, one aspect that has so far been overlooked is the role of moisture during powder storage. Indeed, the reactivity of α-TCP in water makes this issue particularly important, as moisture can potentially alter the powders' reactivity and hence the final properties of the set cement. Specifically, a premature hydrolysis of the powder in presence of humidity could compromise the subsequent reactivity of the powder.

The association of moisture with crystalline solids can result in water adsorption, absorption, deliquescence and capillary condensation, this being particularly important in porous solids [18]. Already the mildest interaction, *i.e.* adsorption, where water molecules associate on a materials' surface, can affect the properties of materials [19,20]. In the case of water absorption, since water penetrates the bulk solid structure, changes in the properties of the material are to be expected in the same way as for deliquescence (dissolution of the material in its own sorbed water) and capillary condensation (water condensation inside pores) for water reacting compounds. This was in fact observed in the work by Gbureck et al. [21] who investigated the shelf-life of β-tricalcium phosphate/monocalcium phosphate cement powders when stored in sealed containers at ambient conditions (22 °C, 60% relative humidity) and observed that the powders converted to dicalcium phosphate anhydrous after a few days. They attributed this conversion to a dissolution/precipitation process triggered by the condensation of humidity on the particles' surfaces acting as reaction medium.

All the changes that moisture can bring to crystalline solids become more evident in amorphous compounds due to their greater sorption capacity [22]. Indeed, the higher surface energy and greater molecular disorder in amorphous solids favour water penetration. The present study aims to investigate how ageing of α-TCP powders stored in sealed containers at different relative humidities affect powder reactivity. Dynamic vapor sorption studies were carried out to assess the reversibility of the process. Moreover, the approach used in this study confirms that monitoring the pH of α-TCP slurries is a very sensitive tool to assess small changes in powder reactivity.

2. Materials and methods

2.1. Preparation and characterization of alpha tricalcium phosphate

α-TCP was synthesized by solid state reaction heating in a furnace (Hobersal CRN-58) a 2:1 M ratio of $CaHPO_4$ (Sigma C7263) and $CaCO_3$ (Sigma–Aldrich C4830). The reagents were mixed (WhipMix) and heated in a platinum crucible as follows: the powders were first heated at a 2,5 °C/min rate to 300 °C, left to dwell for 2 h, then heated to 1100 °C at 2,5 °C/min and left to dwell for 2 h and raised up again to 1400 °C at 2,5 °C/min where they were left to dwell for 2 h. Next, the α-TCP was removed from the furnace and rapidly quenched in air to prevent the formation of β-TCP. The α-TCP was then milled using a planetary mill (Pulverisette 6, Fritsch GmbH) with an agate bowl and balls into fine powder. This involved milling the powder with 10 balls (d = 30 mm) at 450 rpm for 60 min, followed by 500 rpm for 40 min, and lastly using 100 balls (d = 10 mm) at 500 rpm for 60 min. Roughly 20 min were left between each stage to allow to cool down before the next stage began. Two separate batches of 150 g of α-TCP each were made. As a control to test how the presence of the seed affects reactivity, one batch was left without seed (NS), whilst to the other batch 2 wt% of precipitated hydroxyapatite (Alco ref. 1.02143) was added which acted as seed (S). The powder was then kept in a desiccator until use. The seed was expected to act as a nucleating agent for the formation of CDHA during the cement setting reaction.

The particle size distribution upon milling was determined by laser diffraction (Mastersizer 3000, Malvern Instruments, UK) using 96% ethanol as dispersant. The particle refraction and absorption indices were set to 1.63 and 0.1 respectively.

2.2. Moisture adsorption tests

The moisture adsorption on the powders was investigated under static and dynamic conditions at room temperature for different periods of time depending on the experiment. In the former method a closed jar with the relative humidity (RH) of interest was used. This configuration has the advantage of simplicity but the disadvantage of exhibiting longer sorption times to reach equilibrium since only the Brownian movement of the gas was involved in the sorption process. Experiments performed in the closed jars were conducted for time periods that ranged from several days up to 20 weeks depending on the type of experiment as will be explained in the following sections. For the dynamic studies a Dynamic Vapor Sorption device (DVS) was used. In a DVS instrument there is vapor constantly flowing with the help of a gas carrier, thus allowing a faster equilibration. In addition, the DVS instrument incorporates a microbalance to constantly monitor the weight of the sample during analysis, allowing *in situ* weight measurements. The experiments performed by DVS typically lasted 100 min, as it was observed that this time was sufficient for equilibrium conditions to occur.

2.2.1. Moisture adsorption under static conditions

Initially the powders were dried in an oven at 120 °C until they achieved a constant weight (around 2 h). The dry powders were then cooled down in a desiccator and subsequently placed (10–15 g) in sealed containers with different relative humidities (RH). The different RH were attained using selected saturated salt solutions following the ASTM Standard E 104-85 (*Standard practice for maintaining constant relative humidity by means of aqueous solutions*). Specifically: 22,5% RH was created using a saturated solution of potassium acetate (Panreac, 141479.1211), 43,2% RH with potassium carbonate (Emprove, 04924.500), 84,3% RH with potassium chloride (Panreac, 131494.1210) and for 100% RH water was used. At specific time points roughly 1 g of the humidified powder was taken and accurately weighed (hydrated mass, m_h), dehydrated in an oven at 120 °C for 2 h and then kept in a desiccator to cool down before being re-weighed (dried mass, m_d). The difference between weights was expressed as the percentage of water adsorbed by the sample:

$$\%\ adsorbed\ water = \frac{m_h - m_d}{m_d} \times 100 \quad (1)$$

2.2.2. Moisture adsorption under dynamic conditions

Adsorption/desorption isotherms were obtained in a DVS device, consisting in a thermogravimetric balance equipped with a controlled humidity chamber Q500SA Sorption Analyzer (TA Instruments, New Castle, USA). Approximately 60 mg of sample was placed into a sample pan, dried under a nitrogen flow and subsequently brought to different RH ranging from 30 to 98% at 25 °C. Different sorption/desorption experiments were done to assess the reversibility of the process.

The different codes to identify the experiments are.

- powder incorporating seed: S (seed)
- powder without seed: NS (no seed)
- dehydrated powder (120 °C, 2 h): D (dehydrated)
- thermally treated powder (600 °C, 1 h): 600 °C
- power subjected to specific RH (22,5/43,2/84,3/100%) is rounded and named as 20RH, 40RH, 80RH and 100RH.

2.3. Characterization of the powder

2.3.1. Powder reactivity

The reactivity of the powders, before and after the sorption studies, was analysed preparing a slurry and monitoring the pH (Crison GLP 22). The slurry was made using 1 g of α-TCP in 20 ml of deionised water, which was maintained at 38 °C using a jacketed reaction vessel connected to a constant temperature water bath (Huber Kältemaschinenbau

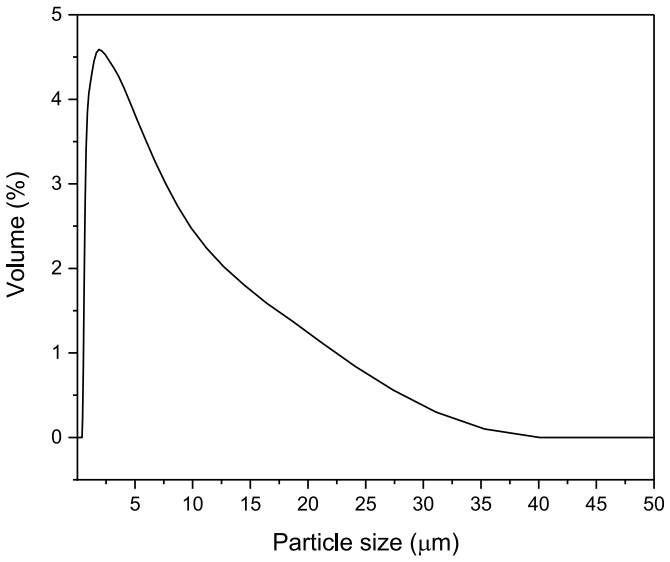

Fig. 1. Particle size distribution of the synthesized α-TCP powder after milling.

GmbH, Germany). The slurry was continuously stirred using a Teflon-coated stir bar. The pH was measured every minute with a glass electrode. At selected times the slurry was removed, and the reaction stopped by centrifugation to isolate the powder from water. Subsequently, the solids were rinsed twice with ethanol, centrifuged again and kept in a desiccator until use.

2.3.2. Phase composition

X-ray diffraction analyses (XRD) were performed in a D8 Advance Diffractometer (Bruker, Karlsruhe, Germany) to check the composition of the powders. The diffractometer equipped with a CuKα X-ray tube was operated at 40 kV and 40 mA. Data were collected in 0,02° steps over the 2θ range of 10°–60° with a counting time of 2 s per step. The content of amorphous phase was quantified by the internal standard method using alpha-alumina (purity 99,99%, Taimicron). Phase quantification was carried out by Rietveld refinement using Profex 4.0.3 as refinement software [23]. The following formula was used for the amorphous calcium phosphate (ACP) quantification:

$$ACP\% = \frac{100}{100 - Q_A} \times 100 \times \left(1 - \frac{Q_A}{Q_M}\right) \quad (2)$$

Where Q_A is the percentage of internal standard added and Q_M is the percentage of internal standard calculated in the Rietveld refinement [24]. For the refinement, the following structures from the Joint Committee on Powder Standards Diffraction were used: 9–432 (CDHA, $Ca_9(HPO_4)$ $(PO_4)_5(OH)$), 9–348 (α-TCP, $Ca_3(PO_4)_2$) and 04-004-2852 (α-Al_2O_3). Moreover, the peak shape was refined by the parameters k2 (micro-strain) which was refined isotropically and the parameter B1 (crystallite size) was refined anisotropically. Additionally, the parameter GEWICHT which controls texture (preferred orientation) was refined increasing the parameter to SPHAR6. Refinement was considered complete when changing the above parameters no longer improved the fit. The parameter k1 which modifies the crystallite size distribution was not refine.

2.3.3. Thermal analysis

Thermal behaviour of the powders was determined using differential

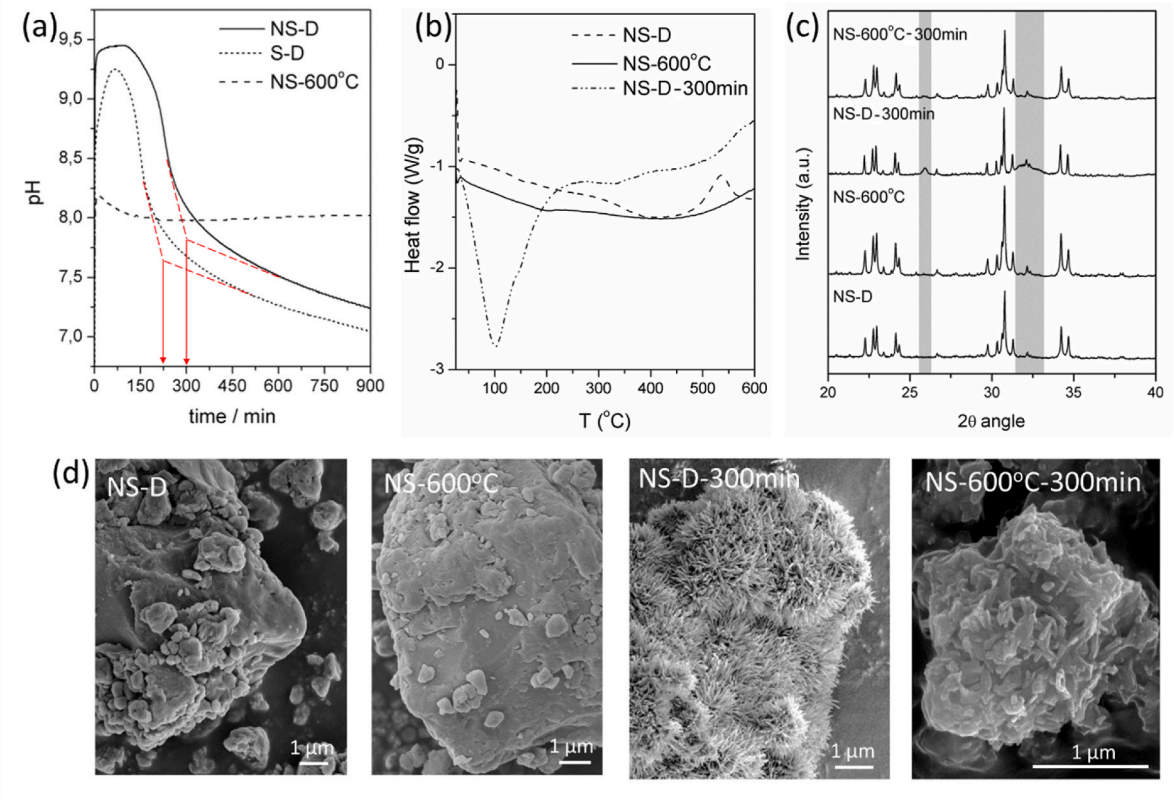

Fig. 2. a) pH profiles of slurries prepared using α-TCP powder without seed (no seed: NS) and dehydrated (NS-D), with seed and dehydrated (S–D) and using powder without seed subjected to a thermal treatment to 600 °C (NS-600 °C). The red arrow indicates the time taken for ACP to hydrolyse, b) DSC analysis of NS-D, NS-600 °C powders, and the NS-D powder isolated from its corresponding slurry after 300 min reaction (NS-D-300min), c) XRD of NS-D and NS-600 °C as-prepared powders and the same powders isolated from their corresponding slurries after 300 min reaction and d) SEM micrographs of the surface of the powders from c). (For interpretation of the references to colour in this figure legend, the reader is referred to the Web version of this article.)

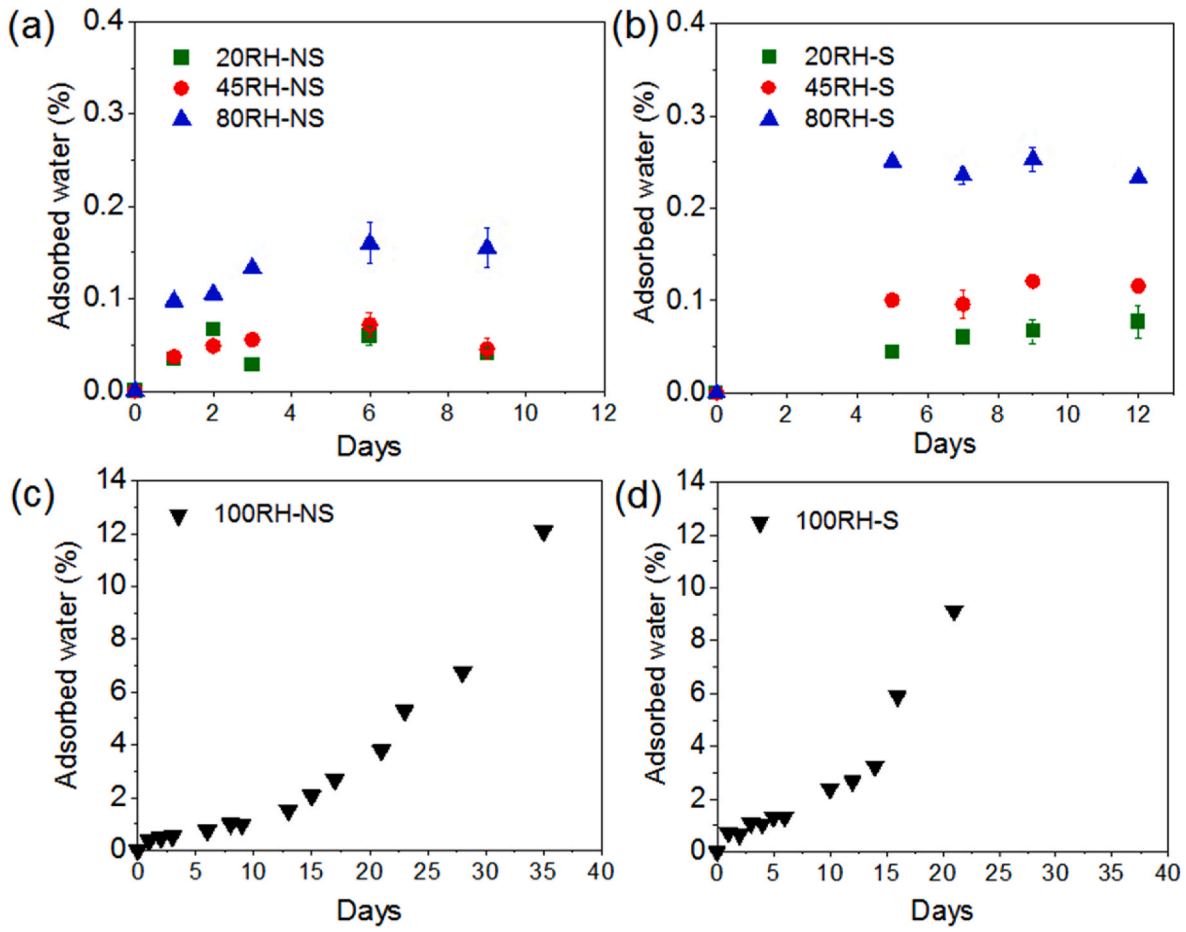

Fig. 3. Water adsorption curves obtained for the NS (a, c) and S (b, d) powders subjected to different moist conditions (a, b) ~20, 40, 80% RH and (c, d) 100% RH under static conditions at room temperature.

scanning calorimetry (DSC, TA 2920). The powder, between 10 and 15 mg, was placed in aluminum pans, crimped using an automated press and subjected to a heating rate of 10 °C/min up to 600 °C in a nitrogen atmosphere.

2.3.4. Surface microstructure

The surface structure of the particles was visually assessed using scanning electron microscopy (SEM, Zeiss Neon 40 SEM) after coating the samples with a thin layer of gold-palladium.

2.3.5. Specific surface area

The SSA was determined by nitrogen adsorption using the Brunauer–Emmett–Teller (BET) method (ASAP 2020, Micrometrics Instrument Corp, Norcross, GA). Before the measurement the samples were outgassed in vacuum conditions (10 mmHg) at a holding temperature of 120 °C.

3. Results and discussion

3.1. Characteristics of the reactivity of the starting powder

The size distribution of α-TCP powder after milling is shown in Fig. 1. The percent of the volume of distribution that lies below the 10, 50 and 90% of the population is: Dv10 = 0.9, Dv50 = 2.89, Dv90 = 12.5 μm.

Monitoring the pH of the slurry proved to be a simple and sensitive test to validate the reactivity of the powders, particularly after moisture adsorption. Indeed, other researchers earlier reported the usefulness of pH monitoring to assess the progress of the setting reaction of cements and particularly for α-TCP hydration [25]. Based on those studies we adapted the settings to monitor the reactivity of α-TCP.

Fig. 2a depicts the pH profiles obtained at 38 °C of slurries prepared with the following powders: powder with/without seed (S/NS) which was dehydrated (D) to remove any trace of moisture (*i.e.* S-D and NS-D respectively), and NS-D powder subjected to thermal treatment at 600 °C (NS-600 °C). The profiles were totally different. While the as-prepared NS and S powders showed an initial pH raise to 9.5 and 9.2 respectively, followed by a steep drop to pH 8.0 and a continuous decrease in pH, the thermally treated powder barely showed any pH change (value around 8) apart from a slight increase at the beginning. The marked increase in pH observed for S-D and NS-D is associated with the dissolution of the powder and the simultaneous uptake of protons by the phosphate PO_4^{3-} into HPO_4^{2-} and $H_2PO_4^-$ in agreement with the observation of other authors [11]. Previous works have also reported that the final pH value characteristic of complete conversion to CDHA oscillates around pH 6 [26]. This implies that the hydrolysis reaction of α-TCP to CDHA should then be characterised by a continuous pH drop [25,26] and failure to see this would indicate that the reaction is not taking place or that the rate of hydrolysis is extremely low [11]. Indeed, the XRD taken after 300 min of reaction of a slurry prepared with the thermally treated powder (Fig. 2c) showed an identical pattern as the starting powder prior to hydrolysis (NS-D) demonstrating that the reaction did not progress. However, the XRD of a NS-D slurry after 300 min of hydrolysis proved that CDHA began to form as observed from the "hump" growing around 31° and the peak appearing at 26°. This difference in reactivity was attributed to the presence of an amorphous phase on the NS-D powder which was formed during the milling protocol. Indeed many authors have proved that extensive and intensive milling of α-TCP powder causes amorphization of the powder [15–17,

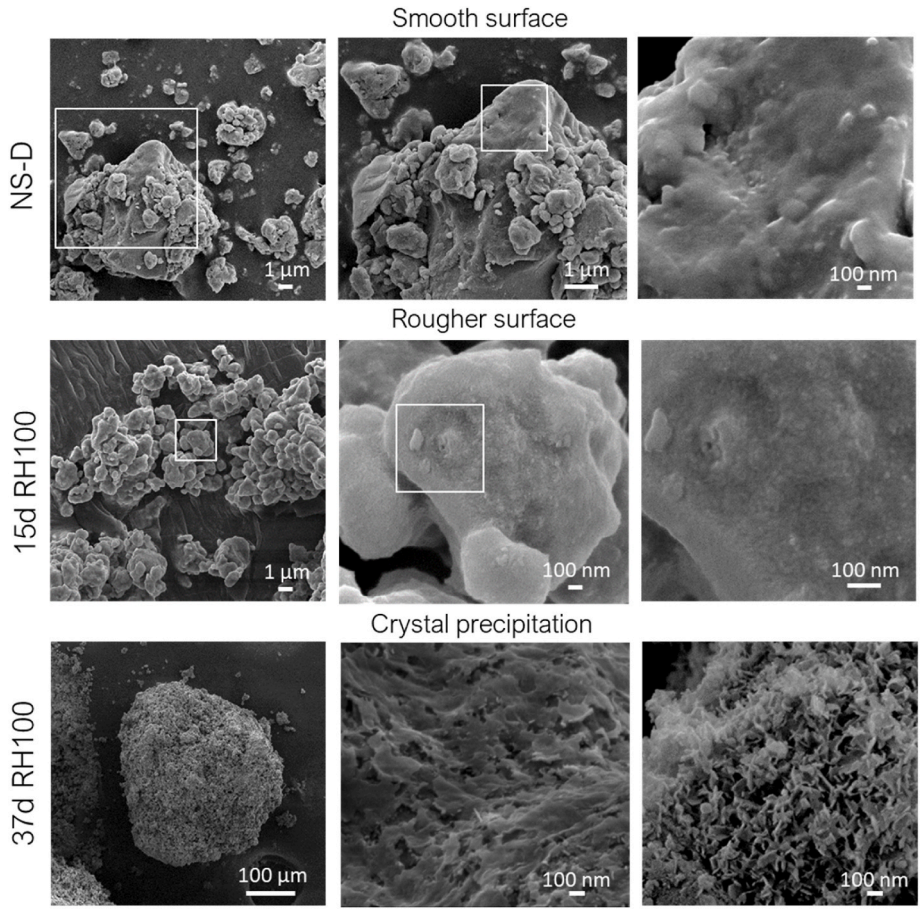

Fig. 4. Microstructure of the surface of the powders observed by SEM taken at different magnifications for the following conditions: as-prepared NS-D powder, NS-D powder subjected to 15d of moist conditions at 100RH at room temperature and NS-D powder subjected to 37d of moist conditions at 100RH at room temperature.

26,27]. The content of amorphous calcium phosphate (ACP) in the milled NS α-TCP powder amounted to 21 wt%. Despite the non-negligible ACP content, this phase was not observed by XRD, where only a general decrease in the intensity of the diffractogram peaks was detected, in line with other published work; in fact, much higher contents are required to translate into appreciable changes - such as the appearance of a "hump" - in the diffractogram. The presence of the amorphous phase was confirmed subjecting the as-prepared powder to a heating cycle up to 600 °C in a differential scanning calorimeter (Fig. 2b) and the exothermic peak observed at ~530 °C was assigned to recrystallisation of the amorphous phase [15,28]. As expected, this peak was not observed on the thermally treated powder proving that heat treatment of the milled NS powder at 600 °C recrystallised the amorphous phase. Further analysis of the pH and DSC profiles in Fig. 2a and b for the different powders, allows associating the reactivity of the amorphous phase to the initial changes in the pH profile (i.e. the first 300 min for NS-D and the first 200 min for S-D) characterised by the fast pH rise and the steep pH drop observed at the beginning of the profiles. This was verified through DSC of the NS-D powder hydrolysed for 300 min (NS-D_300min). The lack of recrystallisation peak confirmed that after 300 min of hydrolysis all the amorphous phase had transformed. These results were in agreement with the works by Hurle et al. [17,29] where they proved that ACP reacted earlier than crystalline α-TCP by *in situ* XRD investigations of the hydration process [16].

Furthermore, SEM images of the microstructure of the particles kept in the slurry for 300 min confirmed the reactivity of NS-D powder, observed by the formation of nanometric needle-shaped crystals on the surface of the powder (Fig. 2d). The formation of these nanometric crystals also explains the broad endothermic peak around 100 °C in the DSC curve of NS-D_300min that accounts for the dehydration of the crystals. In contrast, the microstructure of the powder heat-treated at 600 °C after hydration was hardly altered compared to the microstructure of the pristine NS-600 °C powder, demonstrating its low reactivity (Fig. 2d).

An additional aspect worth noting from the pH profiles was the "progress" of the hydrolysis reaction for powders without ACP (NS-600 °C) or for powders after ACP hydrolysis (e.g. NS-D after 300 min). In the former case the pH profile remained flat while in the latter case the pH curve showed a continuous pH decrease. This different behaviour can be explained by the presence of defects in the lattice of α-TCP in the NS-D powder due to the milling step but also to the presence of newly formed CDHA after 300 min which could act as a seed, i.e. as a substrate for heterogeneous nucleation, accelerating the nucleation reaction and subsequent crystal growth [10,30].

The accelerating effect of the seed is also visible adding commercially available hydroxyapatite to the cement formulation. Indeed, the incorporation of a 2 wt % precipitated hydroxyapatite with a high SSA (in this case of 65,58 m^2/g) in the α-TCP powder is a common strategy to accelerate the hydrolysis reaction [10,26,31]. Both, the stable nature of the seed (i.e. hydroxyapatite) and its elevated surface area favours heterogeneous nucleation and improves the overall reactivity. This is in fact reflected in Fig. 2a where the curve corresponding to the pH profile for the S-D powder proved a faster reactivity of the amorphous phase compared to the NS-D condition. In fact, the amorphous fraction in the NS-D powder took approximately 300 min to hydrolyse while less than 200 min were needed in the presence of seed (S-D).

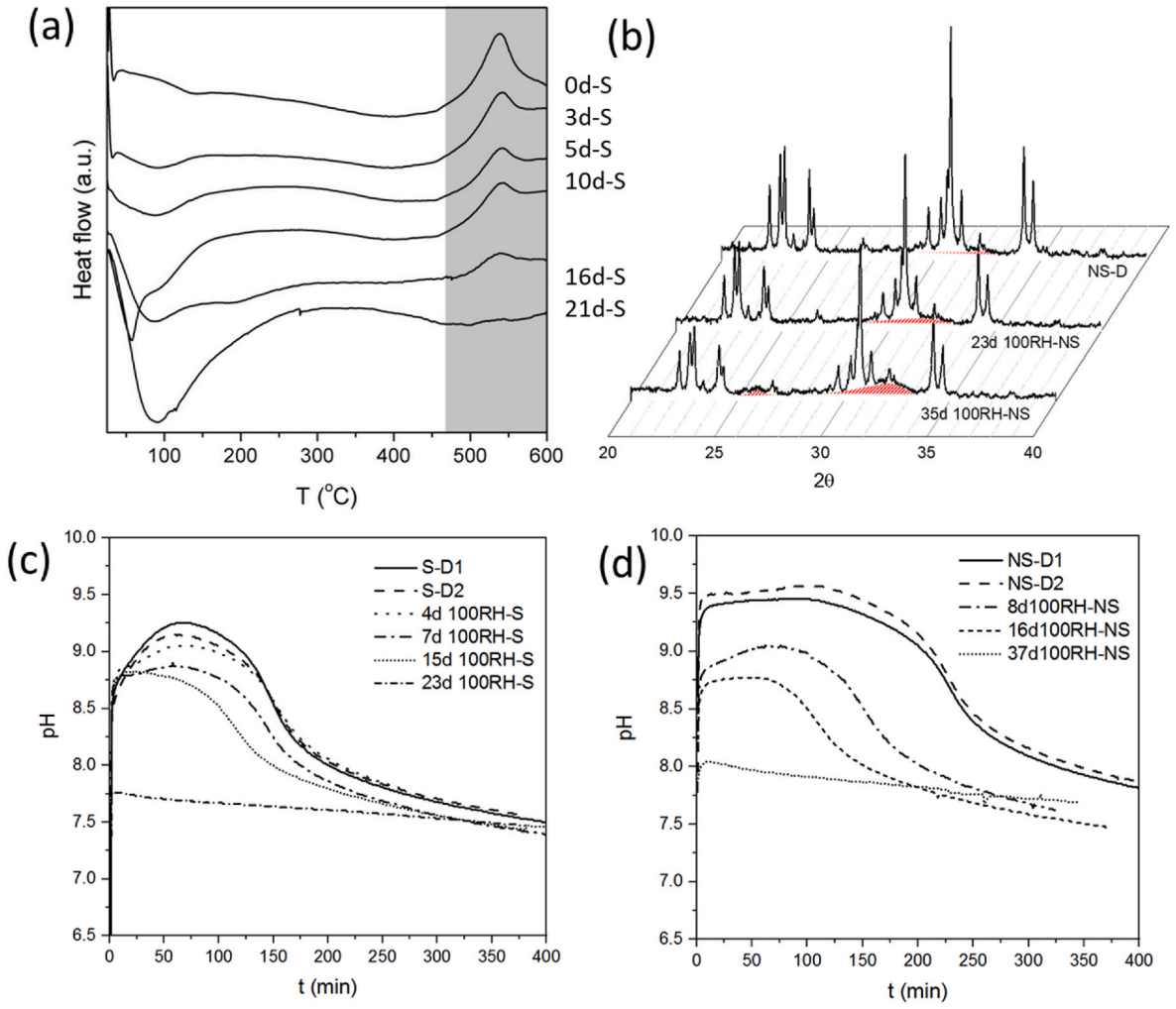

Fig. 5. (a) DSC analysis of S powder that has been previoulsy incubated in moist conditions at RH100 at room temperature for different days. The grey shaded region highlights the exothermic peak associated to recrystallisation of the amorphous phase. (b) XRD of selected powders before and after moisture incubation. Red shaded regions indicate the position where the major peaks of CDHA appear. (c) and (d) pH profiles of powder slurries prepared using powders previously subjected to different moist conditions.

3.2. Moisture uptake under static conditions

Fig. 3 shows the water sorption curves under static conditions for the α-TCP powder with and without seed at different RH. The curves showed that moisture equilibrium conditions were achieved for all RH $\leq$ 80. Instead, an exponential water uptake profile was observed for the powders placed at 100% RH. The anomalous behaviour at 100% RH was a consequence of capillary condensation triggered by the condensation of water on pores and between particles, which led to the gradual hydrolysis of α-TCP to calcium deficient hydroxyapatite [18]. This gradual transformation of α-TCP with smooth surfaces (Fig. 4, NS-D) to an entangled network of nanometric CDHA crystals (Figs. 4 and 37d_100RH-NS) provides a larger surface area for water sorption (Fig. 4) and therefore to greater percentages of adsorbed water (Fig. 3). Crystal precipitation was however only observed on confined regions where it was easier for water to condense. On more open surfaces it was difficult to detect the precipitation of crystals and only a slight roughening of the particle surface was seen (Figs. 4 and 15d_100RH-NS). Interestingly, the macroscopic observation of the powder as hydration progressed showed a marked agglomeration between particles confirming that water condensation was preferably taking place in the gaps between particles where stronger capillary forces can develop (Fig. 4) [32].

It was also observed from Fig. 3 (curves 45RH and 80RH) that the samples containing 2 wt% of seed almost doubled the amount of moisture weight compared to the NS ones. This was attributed to the presence of seed. Indeed, even if only a 2 wt% was added, the nanometric size of the seed provided a large surface area which greatly contributed to the water sorption process. In fact, comparing the values of SSA obtained for the seed (65,58 m^2/g) and α-TCP NS (2,22 m^2/g), the presence of 2 wt% of seed contributes with 37% to the total SSA which is rather consistent with the increase in the percentage of adsorbed water.

To gain further insights into the reactivity of the powder at 100% RH, additional experiments by differential scanning calorimetry were made allowing to monitor the consumption of the amorphous fraction with time (Fig. 5). The gradual decrease in enthalpy associated with recrystallisation of the amorphous phase (peak at ~530 °C) with time pointed towards hydrolysis of this phase at 100% RH and the simultaneous precipitation of CDHA nanocrystals, as indirectly observed by the broad endothermic peak around 100 °C associated with crystal dehydration (Fig. 5a). In addition, the results by XRD of the powder subjected to moisture (Fig. 5b) confirmed the gradual precipitation of CDHA. Indeed, the broad peaks centred at 26° and 32° accounted for the precipitation of very small crystals of CDHA. Regarding the pH profiles of the slurries with powder subjected to 100% RH, it is observed that the ACP fraction takes progressively less time to transform (Fig. 5c and d). This can be explained by the presence of CDHA already in the powder, which acts as

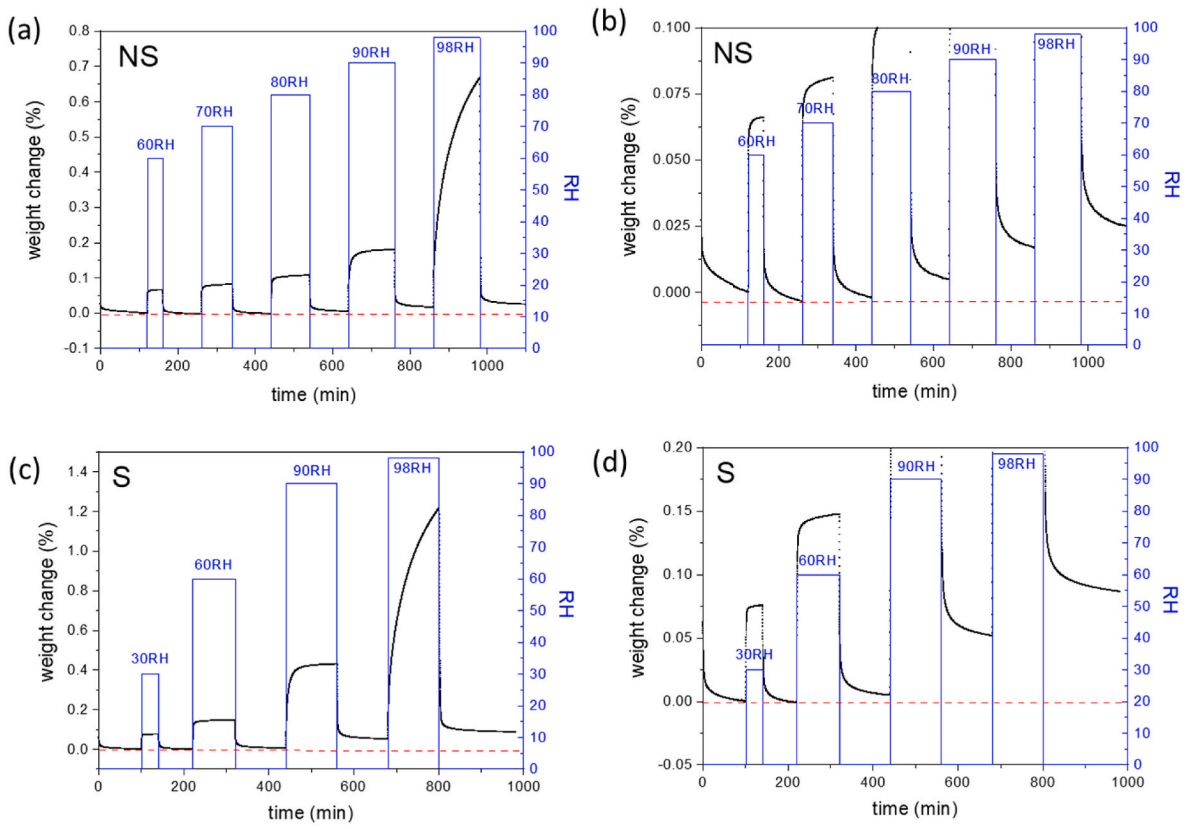

Fig. 6. DVS profiles monitoring the weight change of the powders when submitting them to controlled moisture cycles: (a, b) NS powders and (c, d) S powder. (a, c) Overall plot, (b,c) closer look of the weight changes during the desorption step. The blue solid line shows the humidity cycles performed while the black line registers the associated weight changes. The red-dotted line was drawn to help visualising changes in the weight of the powder upon desorption. (For interpretation of the references to colour in this figure legend, the reader is referred to the Web version of this article.)

a seed accelerating the hydrolysis process. However, we cannot exclude the effect of a lower content of ACP remaining in the pre-hydrolysed powder.

3.3. Moisture uptake under dynamic conditions

Fig. 6 shows the sorption profiles obtained through DVS studies to help determining more accurately the water sorption characteristics. This technique allowed to continuously monitor the weight change when submitting the powder to controlled moisture cycles. The blue solid line in the graphs shows the humidity cycles performed while the black line registers the associated weight changes. After every RH equilibration it followed a drying step to assess the reversibility of the water sorption process. Each analysis began by drying the powder under a nitrogen flow and this was followed by the various hydration-dehydration cycles. As expected, similar equilibration curves with comparable water uptake percentages to the ones observed under static conditions (for conditions below 98% RH) were obtained. However, the dehydration step performed after each moisture cycle showed that not all the sorbed water was removed suggesting that a fraction of the sorbed water became very tightly bound or ended up reacting with the powder. This raises the question as to whether this reacted or tightly bound water (i.e. strongly associated with the material) could influence the reactivity of the powder.

3.4. Influence of moisture sorption on powder reactivity

To determine the changes in the reactivity of powder subjected to specific moisture conditions at RH < 100, the pH of the corresponding slurries was monitored as described in section 3.1. Fig. 7 compares the different profiles obtained for the NS-D and S-D powders subjected to 80% RH for different periods of time. Despite the high RH and a relatively long incubation time of 3 weeks, and contrary to what happened to the 100RH samples (Fig. 5), there were no noticeable changes in the reactivity of the amorphous fraction. This was concluded upon observing that the time taken for the amorphous phase to hydrolyse (i.e. 250 min for the powder without seed and around 200 min for the powder with seed) remained unaltered on powders kept at 80% RH for less than 3 weeks. In addition, the pH profiles of powders subjected to moisture (<3 weeks) but subsequently dehydrated presented an almost identical pH profile to that of the as-prepared powders suggesting that under static conditions water sorption was not influencing reactivity.

Differences in the pH profiles were however observed on powders subjected to long incubation times as observed in the pH profiles obtained at e.g. 12 and 20 weeks for the NS and S powders respectively (Fig. 7). The amorphous fraction required less time to transform, indicating a faster reactivity. This can be explained if a prehydrolysis similar to that observed for 100RH occurs during powder storage (Fig. 5). In fact, the formation of CDHA is expected to act as a seed that accelerates the reaction. To check whether partial hydrolysis occurred during storage of the powder in RH80 (Fig. 7), XRD analyses were performed (Fig. 8). Fig. 8 compares the XRD of the as-prepared NS powder with the same powder subjected for 12 weeks to moisture at a 80% RH. Although no distinct CDHA peaks were found to justify the transformation of the amorphous phase to crystalline CDHA, the diffractogram clearly showed a decrease in the intensity of the α-TCP peaks after incubation, which we associate to the hydrolysis of this phase to a probably amorphous calcium phosphate. In fact, this decrease was also observed in samples incubated at 100RH, however, in that case it was associated with the hydrolysis of α-TCP to CDHA. The fact that we now do not "yet" see

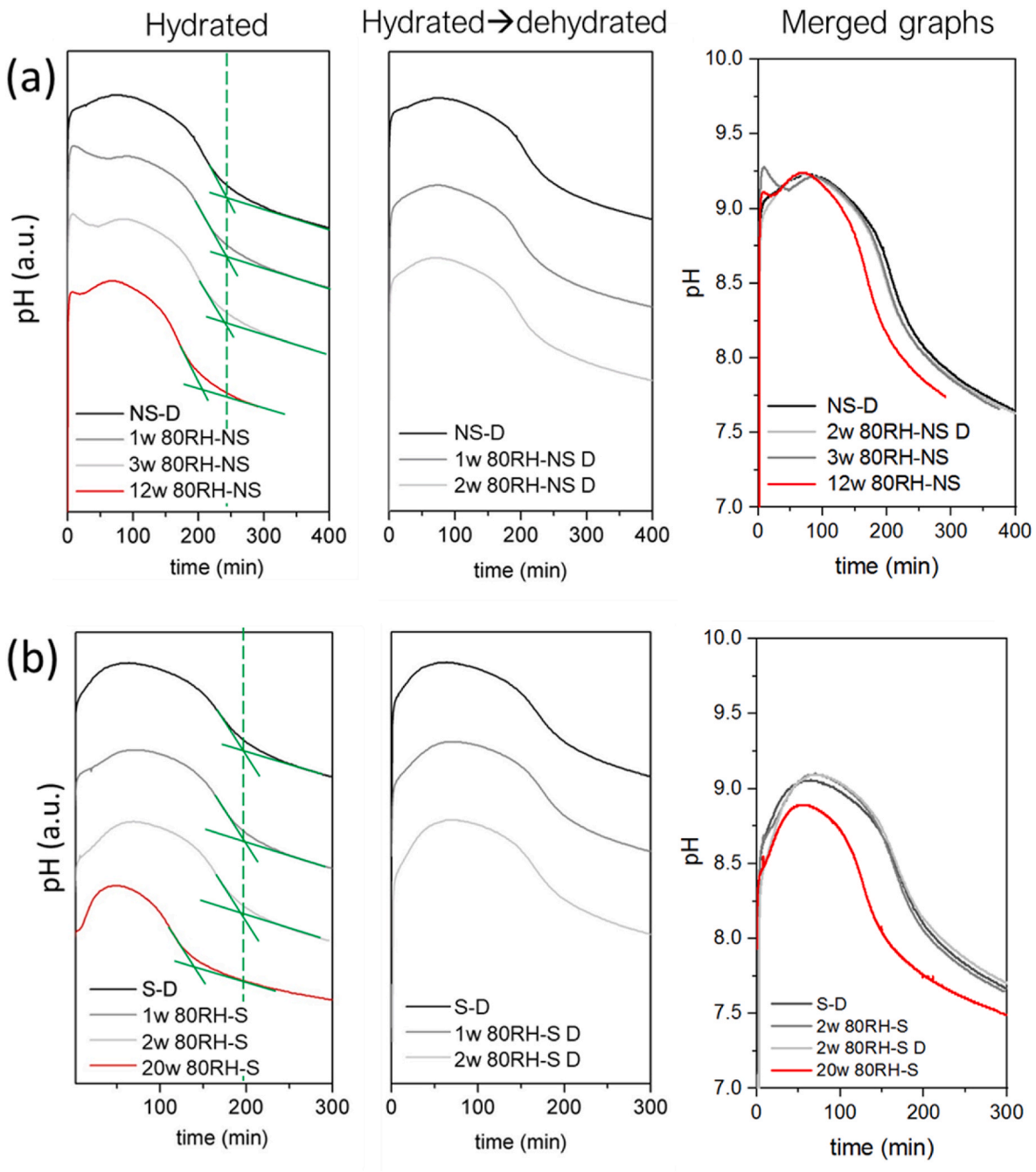

Fig. 7. Representative pH profiles of slurries prepared using NS powders (a), and S powders (b). Prior to pH monitoring the powders were subjected to incubation in different moisture conditions (graph legend).

CDHA we believe is due to the less efficient hydrolysis at 80RH compared to 100RH, where in the latter case water condensation occurs.

The overall results demonstrate that, despite the inherent affinity of milled α-TCP powder for water, moisture uptake under high relative humidity conditions did not appear to compromise the reactivity of the powder in the three weeks of incubation at 80% RH, although it did for longer incubation times. Further studies would be needed to disclose the long-term stability of the powder and provide the shelf-life for this type of materials.

4. Conclusions

The results of the present study shed light on the moisture degradation of α-TCP powders. Despite the high affinity for water and the presence of a highly reactive amorphous phase created during milling, studies conducted under static conditions showed that in the tested powder, for at least three weeks, the reactivity of the powder remained unchanged when stored at 80% RH at room temperature. This was concluded by analyzing the evolution of the pH curves of the powder slurries, together with morphological, structural and thermal analyses performed on the powders. However, it was also shown that longer incubation times at 80% RH eventually affected the reactivity of the powders. Although changes in reactivity were only visible after long incubation times, dynamic sorption studies revealed that shortly after the water adsorbed on the powder surface, a fraction of the adsorbed water was irreversibly bound. Thus, static and dynamic sorption studies demonstrate that despite water sorption takes place irreversibly, these changes only alter reactivity after long incubation times. This work

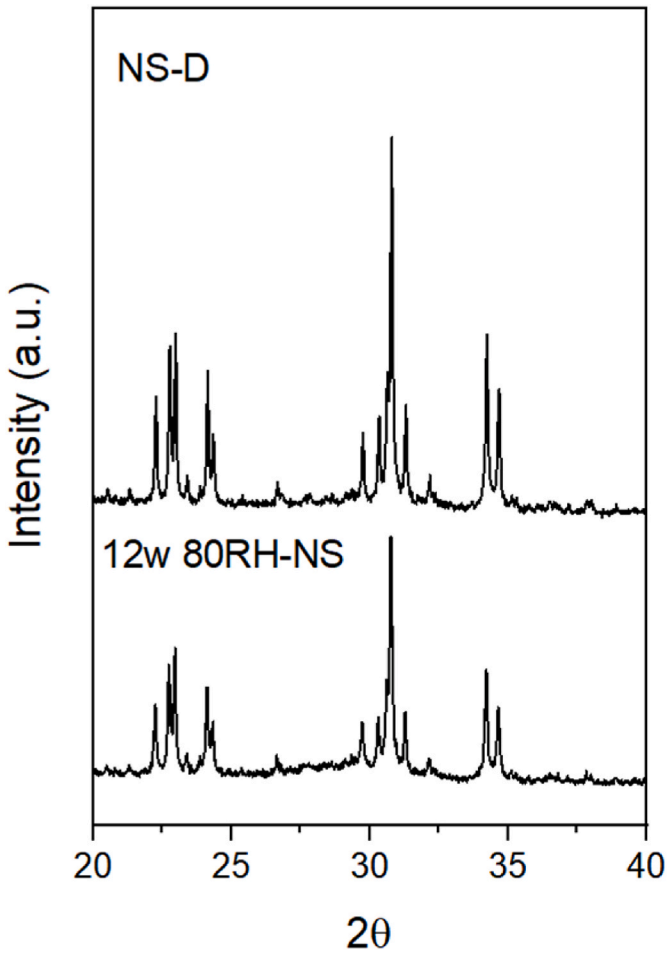

Fig. 8. XRD of the as-prepared NS-D powder and NS powder stored for 12 weeks at a 80% RH at room temperature. All the peaks were assigned to α-TCP with JCPDS 9–348.

highlights the effectiveness of simple tools, such as pH monitoring of a slurry, to detect fine changes in powder reactivity that could affect its performance as a main component of hydraulic cements and self-setting inks.

Notes

The authors declare no competing financial interest.

Declaration of competing interest

The authors declare that they have no known competing financial interests or personal relationships that could have appeared to influence the work reported in this paper.

Acknowledgment

Authors acknowledge the Spanish Government for financial support through the PID2019-103892RB-I00 project. They also thank the Generalitat de Catalunya for funding through projects 2017SGR-1165 and BASE3D 001-P-001646 (co-funded by the European Regional Development Fund). MPG acknowledges the ICREA Academia award and ME the Serra Hunter Fellowship, both from the Generalitat de Catalunya.

References

[1] H.F. Albee, F.H. Morrison, Studies in bone growth: triple calcium phosphate as a stimulus to osteogenesis, Ann. Surg. 70 (1920) 32–39.
[2] M.-P. Ginebra, E. Fernández, F.C.M. Driessens, J.A. Planell, Modeling of the hydrolysis of α-tricalcium phosphate, J. Am. Ceram. Soc. 82 (1999) 2808–2812, https://doi.org/10.1111/j.1151-2916.1999.tb02160.x.
[3] F.C.M. Driessens, M.G. Boltong, O. Bermudez, J.A. Planell, M.P. Ginebra, E. Fernandez, Effective formulations for the preparation of calcium phosphate bone cements, J. Mater. Sci. Mater. Med. 5 (1994) 164–170, https://doi.org/10.1007/BF00053338.
[4] Y. Maazouz, E.B. Montufar, J. Guillem-Marti, I. Fleps, C. Öhman, C. Persson, M. P. Ginebra, Robocasting of biomimetic hydroxyapatite scaffolds using self-setting inks, J. Mater. Chem. B. 2 (2014) 5378, https://doi.org/10.1039/C4TB00438H.
[5] Y. Maazouz, E.B. Montufar, J. Malbert, M. Espanol, M.-P. Ginebra, Self-hardening and thermoresponsive alpha tricalcium phosphate/pluronic pastes, Acta Biomater. 49 (2017) 563–574, https://doi.org/10.1016/j.actbio.2016.11.043.
[6] A. Barba, A. Diez-Escudero, Y. Maazouz, K. Rappe, M. Espanol, E.B. Montufar, M. Bonany, J.M. Sadowska, J. Guillem-Marti, C. Öhman-Mägi, C. Persson, M.-C. Manzanares, J. Franch, M.-P. Ginebra, Osteoinduction by foamed and 3D-printed calcium phosphate scaffolds: effect of nanostructure and pore architecture, ACS Appl. Mater. Interfaces 9 (2017) 41722–41736, https://doi.org/10.1021/acsami.7b14175.
[7] M.P. Ginebra, E. Fernandez, E.A. De Maeyer, R.M. Verbeeck, M.G. Boltong, J. Ginebra, F.C. Driessens, J.A. Planell, Setting reaction and hardening of an apatitic calcium phosphate cement, J. Biomater. Appl. 76 (1997) 905–912, https://doi.org/10.1177/0022034597076041201.
[8] M. Bohner, Reactivity of calcium phosphate cements, J. Mater. Chem. 17 (2007) 3980, https://doi.org/10.1039/b706411j.
[9] M. Bohner, R. Luginbuhl, C. Reber, N. Doebelin, G. Baroud, E. Conforto, A physical approach to modify the hydraulic reactivity of alpha-tricalcium phosphate powder, Acta Biomater. 5 (2009) 3524–3535, https://doi.org/10.1016/j.actbio.2009.05.024.
[10] C. Liu, W. Shen, Effect of crystal seeding on the hydration of calcium phosphate cement, J. Mater. Sci. Mater. Med. 8 (1997) 803–807. http://www.ncbi.nlm.nih.gov/pubmed/15348795.
[11] T. Martinez, M. Espanol, C. Charvillat, O. Marsan, M.P. Ginebra, C. Rey, S. Sarda, A-tricalcium phosphate synthesis from amorphous calcium phosphate: structural characterization and hydraulic reactivity, J. Mater. Sci. 56 (2021) 13509–13523, https://doi.org/10.1007/s10853-021-06161-0.
[12] C. Durucan, P.W. Brown, Kinetic model for α-tricalcium phosphate hydrolysis, J. Am. Ceram. Soc. 85 (2002) 2013–2018, https://doi.org/10.1111/j.1151-2916.2002.tb00397.x.
[13] M.P. Ginebra, F.C.M. Driessens, J.A. Planell, Effect of the particle size on the micro and nanostructural features of a calcium phosphate cement: a kinetic analysis, Biomaterials 25 (2004) 3453–3462.
[14] U. Gbureck, J.E. Barralet, L. Radu, H.G. Klinger, R. Thull, Amorphous a-tricalcium phosphate : preparation and aqueous setting reaction, J. Am. Ceram. Soc. 1132 (2004) 1126–1132.
[15] C.L. Camire, U. Gbureck, W. Hirsiger, M. Bohner, Correlating crystallinity and reactivity in an alpha-tricalcium phosphate, Biomaterials 26 (2005) 2787–2794, isi:000226675500001.
[16] K. Hurle, J. Neubauer, M. Bohner, N. Doebelin, F. Goetz-Neunhoeffer, Effect of amorphous phases during the hydraulic conversion of α-TCP into calcium-deficient hydroxyapatite, Acta Biomater. 10 (2014) 3931–3941, https://doi.org/10.1016/j.actbio.2014.03.017.
[17] K. Hurle, J. Neubauer, M. Bohner, N. Doebelin, F. Goetz-Neunhoeffer, Calorimetry investigations of milled α-tricalcium phosphate (α-TCP) powders to determine the formation enthalpies of α-TCP and X-ray amorphous tricalcium phosphate, Acta Biomater. 23 (2015) 338–346, https://doi.org/10.1016/j.actbio.2015.05.026.
[18] C. Ahlneck, G. Zografi, The molecular basis of moisture effects on the physical and chemical stability of drugs in the solid state, Int. J. Pharm. 62 (1990) 87–95, https://doi.org/10.1016/0378-5173(90)90221-O.
[19] I. Opaliński, M. Chutkowski, A. Hassanpour, Rheology of moist food powders as affected by moisture content, Powder Technol. 294 (2016) 315–322, https://doi.org/10.1016/j.powtec.2016.02.049.
[20] B. Armstrong, K. Brockbank, J. Clayton, Understand the effects of moisture on powder behavior, Chem. Eng. Prog. 110 (2014) 25–30.
[21] U. Gbureck, S. Dembski, R. Thull, J.A. Barralet, Factors influencing calcium phosphate cement shelf-life, Biomaterials 26 (2005) 3691–3697.
[22] S. Airaksinen, M. Karjalainen, A. Shevchenko, S. Westermarck, E. Leppänen, J. Rantanen, J. Yliruusi, Role of water in the physical stability of solid dosage formulations, J. Pharmacol. Sci. 94 (2005) 2147–2165, https://doi.org/10.1002/jps.20411.
[23] N. Doebelin, R. Kleeberg, Profex: a graphical user interface for the Rietveld refinement program BGMN, J. Appl. Crystallogr. 48 (2015) 1573–1580, https://doi.org/10.1107/S1600576715014685.
[24] H.P.T. Westphal, T. Füllmann, Rietveld quantification of amorphous portions with an internal standard—mathematical consequences of the experimental approach, Powder Diffr. 24 (2009) 239–243.
[25] K. TenHuisen, Formation of calcium-deficient hydroxyapatite from α-tricalcium phosphate, Biomaterials 19 (1998) 2209–2217, https://doi.org/10.1016/S0142-9612(98)00131-8.
[26] C. Durucan, W.E. Brown, Reactivity of alpha-tricalcium phosphate, J. Mater. Sci. 37 (2002) 963–969, isi:000174853200009.

[27] T.J. Brunner, R.N. Grass, W.J. Stark, Effect of particle size , crystal phase and crystallinity on the reactivity of tricalcium phosphate cements for bone reconstruction, J. Mater. Chem. 17 (2007) 4072–4078, https://doi.org/10.1039/b707171j.

[28] C.F. Feng, K.A. Khor, S.W.K. Kweh, P. Cheang, Thermally induced crystallization of amorphous calcium phosphate in plasma-spheroidised hydroxyapatite powders, Mater. Lett. (2000) 229–233.

[29] K. Hurle, J. Neubauer, F. Goetz-Neunhoeffer, Hydration enthalpy of amorphous tricalcium phosphate resulting from partially amorphization of β-tricalcium phosphate, BioNanoMaterials 18 (2017), https://doi.org/10.1515/bnm-2016-0016.

[30] K. Tsuru, Ruslin, M. Maruta, S. Matsuya, K. Ishikawa, Effects of the method of apatite seed crystals addition on setting reaction of α-tricalcium phosphate based apatite cement, J. Mater. Sci. Mater. Med. 26 (2015) 1–8, https://doi.org/10.1007/s10856-015-5570-8.

[31] E. Fernandez, M.P. Ginebra, M.G. Boltong, F.C.M. Driessens, J.A. Planell, J. Ginebra, E.A.P. De Maeyer, R.M.H. Verbeeck, Kinetic study of the setting reaction of a calcium phosphate bone cement, J. Biomed. Mater. Res. 32 (1996) 367–374, https://doi.org/10.1002/(SICI)1097-4636(199611)32:3<367::AID-JBM9>3.0.CO;2-Q.

[32] E. Charlaix, M. Ciccotti, Capillary condensation in confined media, in: K. Sattler (Ed.), Handb. Nanophysics Princ. Methods, CRC Press, Boca Raton, FL, 2010. http://arxiv.org/abs/0910.4626.